Carbohydrate Polymers 114 (2014) 506–513

Contents lists available at ScienceDirect

Carbohydrate Polymers

journal homepage: www.elsevier.com/locate/carbpol

Rheological behaviors of an exopolysaccharide from fermentation medium of a *Cordyceps sinensis* fungus (Cs-HK1)

Fengyuan Sun[a], Qilin Huang[a,*], Jianyong Wu[b]

[a] College of Food Science and Technology, and MOE Key Laboratory of Environment Correlative Dietology, Huazhong Agricultural University, Wuhan 430070, China
[b] Department of Applied Biology & Chemical Technology, The Hong Kong Polytechnic University, Hung Hom, Kowloon, Hong Kong

ARTICLE INFO

Article history:
Received 9 July 2014
Received in revised form 21 August 2014
Accepted 23 August 2014
Available online 29 August 2014

Keywords:
Exopolysaccharide
Rheological behaviors
Cordyceps sinensis

ABSTRACT

The rheological behaviors of an exopolysaccharide (EPS) from a *Cordyceps sinensis* fungus fermentation were investigated. The intrinsic viscosity of 1986 ± 55 mL/g indicated an extended and rigid chain for EPS. Shear-thinning behavior was observed and became apparent with increasing concentration. According to cross model, two critical transition concentrations (c^* and c^{**}) from dilute solution to semidilute and then to concentrated domain were 0.45 and 6.14 mg/mL. Flow activation energy was calculated by Arrhenius equation and decreased with increasing concentration, indicating a lower sensitivity to temperature. From dynamic frequency sweep, EPS system was classified to three regions including dilution solution (1.25 mg/mL), entanglement network (3.75 and 5.00 mg/mL) and weak gel (≥7.50 mg/mL). Notably, the increase in η^* at high frequencies was attributed to a large flow resistance depended on the rigid chain of EPS. Based on Winter–Chambon criterion, EPS formed gel at 2.6 mg/mL (c_{gel}) and showed typical weak gel from temperature ramp and repetitive strain sweep.

1. Introduction

Cordyceps sinensis, generally known as the Chinese caterpillar fungus, has been used extensively as a folk tonic food and traditional Chinese medicine over the past 300 years for a broad spectrum of health benefits and pharmacological functions (Zhao, Xie, Wang, & Li, 2014). At present, wild *C. sinensis* has become increasingly scarce owing to reckless harvesting and harsh conditions for its growth, which makes wild *C. sinensis* become increasingly expensive. Therefore, a great commercial importance has been attracted to mycelial fermentation to produce *C. sinensis* and its biological components because of its economy and high yield. Polysaccharides are dominant and high bioactive compounds in *C. sinensis*, and have attracted extensive attention due to their various bioactivities, complex structures, extensive adaptability and high content in *Cordyceps* (Wu et al., 2014; Yan, Wang, & Wu, 2014). In our previous studies, Cs-HK1, a *C. sinensis* species, was isolated from a natural fruiting body, and Cs-HK1 mycelial fermentation has produced a large amount of exopolysaccharide (EPS, 4–5 g/L). EPS is a water-soluble polysaccharide secreted by Cs-HK1 to the outside of cell wall in the metabolic process. It can be isolated and purified from fermentation media easily by graded ethanol precipitation; meanwhile, it exhibits significant antioxidant and immunomodulatory activities (Huang, Siu, Wang, Cheung, & Wu, 2013; Wang et al., 2011a,b). Hence, the EPS from Cs-HK1 fermentation medium has a good prospect of application as a functional food and natural drug.

As important characteristics of polysaccharides, rheological behaviors not only have great influences on the manufacture, storage, and texture properties of polysaccharides as food or medicine, but also have internal relations to the molecular structure and chain conformation (Huang, Huang, Li, & Zhang, 2009; Xu, Xu, Zhang, & Zhang, 2008). Thereby, a thorough understanding of the rheological behaviors of polysaccharides is of theoretical and practical value. Curdlan is widely used as a food additive for its unique ability to form either thermo-reversible hydrogels (<60 °C) or thermo-irreversible ones (>80 °C) depending on heating temperatures alone. The rheological behaviors of curdlan are also strongly related to the solvent. Namely, curdlan may exist as a triple helix in water so as to have a high viscosity, while it is unspiraled to single coil in DMSO, so that its viscosity shows a sharp drop (Zhang & Nishinari, 2009). It was reported that *Aeromonas* gum had high intrinsic viscosity, but could not form gel in aqueous system even at high concentration, attributed to its nature of a random coil-like exopolysaccharide (Xu, Chen, & Zhang, 2007). Lentinan can form gel network at low concentration and temperature in water,

* Corresponding author. Tel.: +86 027 87283007; fax: +86 027 87288375.
E-mail address: whuhql@gmail.com (Q. Huang).

http://dx.doi.org/10.1016/j.carbpol.2014.08.055
0144-8617/

which is closely related to its triple-helical conformation (Zhang, Xu, & Zhang, 2008). However, despite various researches carried out on the rheological properties of polysaccharides, the rheological behaviors of EPS from *Cordyceps* mycelia have not been reported yet.

It is well known that polymer solutions can be divided into three concentration regions. In extremely dilute solutions, the polymer coils are separate from each other. The coils begin to overlap and interpenetrate with increasing concentration, and finally form interpenetration network in more concentrated solution; therefore, polymer shows different rheological behaviors in different concentration regions due to the interactions between polymer chains (Zhang, Li, Wang, Zhang, & Cheung, 2011). Hence, in this work, the effects of concentration and temperature on the rheological behaviors of EPS in aqueous solutions were studied systematically by steady shear and dynamic oscillatory tests. In steady shear tests, the critical concentrations from dilute to concentrated solutions were estimated by the concentration dependence of zero-shear viscosity calculated by cross model. In dynamic oscillatory tests, the sol–gel point at critical gelation concentration was determined by Winter–Chambon criterion. The gel properties were evaluated by temperature ramp and repetitive strain sweep. This work will provide comprehensive information on the rheological properties of exopolysaccharides from fermentation medium, and contribute to the production of exopolysaccharides by mycelial fermentation and its application in health care products.

2. Materials and methods

2.1. EPS isolation and solution preparation

The exopolysaccharide (EPS) was isolated and purified by gradient ethanol precipitation from fermentation medium of a *C. sinensis* fungus Cs-HK1 as described in our previous work (Huang et al., 2013). In brief, ethanol (95% grade) was added successively at 1/5, 2/5, 1, 2 and 5 volume ratio to the fermentation medium of Cs-HK1, and the corresponding precipitates were collected by centrifugation and designated as $P_{1/5}$, $P_{2/5}$, P_1, P_2, and P_5, respectively. Among the precipitated fractions, $P_{2/5}$ had a total sugar content of 99% measured by the phenol-sulfuric acid method and a high purity as indicated by a single peak in the gel permeation chromatography (GPC). Therefore, $P_{2/5}$ was identified as the EPS for the present study.

The EPS was dissolved fully in pure water to prepare the mother solution at a concentration of 15 mg/mL. The EPS solutions at different concentrations (0.03–15 mg/mL) were prepared by gradual dilution method.

2.2. Intrinsic viscosity ([η]) by viscometry

The intrinsic viscosities ([η]) of EPS in pure water and 0.2 M NaCl were measured at 25 °C by an Ubbelohde capillary viscometer. The kinetic energy correction was negligible, since the effluent time of the two solvents was always beyond 120 s. Huggins and Kraemer equations were used to estimate [η] by extrapolation to infinite dilution as follows:

$$\text{Huggins}: \frac{\eta_{sp}}{c} = [\eta] + k'[\eta]^2 c \quad (1)$$

$$\text{Kraemer}: \frac{(\ln \eta_r)}{c} = [\eta] + k''[\eta]^2 c \quad (2)$$

where η_{sp}/c is reduced specific viscosity; $(\ln\eta_r)/c$ is inherent viscosity; k' and k'' are constants depending on the molecular properties, solvent and experimental conditions.

2.3. Steady shear test

The EPS solutions at concentrations ranging from 0.03 to 15 mg/mL in pure water were characterized for rheological behaviors by steady shear tests. All measurements were carried out on a Discovery H-2 strain-controlled rheometer (TA Instrument, New Castle, USA) fitted with a cone and plate geometry system (cone: diameter, 40 mm; angle, 2°; gap, 61 μm). The steady shear viscosity (η), as known as the apparent viscosity, was measured in the shear rate (γ) range of 0.1–700 s^{-1}. The data were plotted in a logarithmic scale based on η as a function of γ. All steady shear measurements were repeated three times.

2.4. Dynamic oscillatory test

Dynamic frequency sweeps were performed to determine the values of storage modulus (G'), loss modulus (G'') and complex viscosity (η^*) vs the angle frequency (ω) ranging from 0.1 to 300 rad/s at a fixed strain of 2% and 25 °C. Dynamic temperature ramp tests were done in the temperature range of 4–90 °C with the heating and cooling rate of 5 °C/min at an angle frequency of 1 rad/s and a strain of 2%. Repeated strain sweep measurements were done at 1 rad/s and 25 °C with a strain range from 0.1 to 900%, and the next sweep was started immediately after the previous one was finished. The EPS solution was loaded between cone and plate with a gap of 61 μm at desired temperature and allowed to equilibrate for about 15 min so as to make temperature equilibration and stress relaxation. In order to avoid sample dehydration, the exposed edge was covered with a thin layer of liquid paraffin. All the dynamic measurements were performed in the linear viscoelastic region and repeated three times.

3. Results and discussion

3.1. Determination of intrinsic viscosity

Intrinsic viscosity ([η]) is a fundamental parameter used to represent the hydrodynamic volume occupied by individual macromolecules in dilute solution. For most neutral polysaccharides, Huggins and Kraemer plots have practical advantages in that they normally give linear plots, so they are generally used to estimate the [η] of neutral polysaccharides (Higiro, Herald, & Alavi, 2006). As shown in Suppl. Fig. 1, Huggins and Kraemer plots of EPS all showed linear dependence of concentration in both aqueous media, suggesting a normal viscosity behavior as a neutral polysaccharide. Moreover, [η] obtained from the intercepts of Huggins and Kraemer plots was 1986 ± 55 mL/g in pure water and 1990 ± 175 mL/g in 0.2 M NaCl. No significant difference in [η] confirmed further that EPS was a neutral polysaccharide or nonionic one, since the adding salt did not alter its surface charge characteristics to influence viscosity. The values of [η] for EPS were higher than those of some neutral polysaccharides in aqueous media such as curdlan (527 mL/g), lentinan (903.3 mL/g), konjac glucomannan (1320 mL/g) and *Auricular-judae* glucan (1753 mL/g) (Funami, Funami, Yada, & Nakao, 2000; Xu, Chen, & Zhang, 2007; Yoshimura & Nishinari, 1999; Xu, Xu, & Zhang, 2012). Generally, a larger value of [η] reflects an extended and rigid chain conformation, while a smaller [η] value (≤20 mL/g) suggests compact coil conformation (Huang et al., 2013). Hence, the relatively larger [η] value suggests that EPS existed as an extended and rigid chain in aqueous solution.

3.2. Shear rate and concentration dependence of apparent viscosity in steady shear

Fig. 1 shows the dependence of the apparent viscosity (η) on shear rate (γ) for EPS at various concentrations (c) and 25 °C. The η

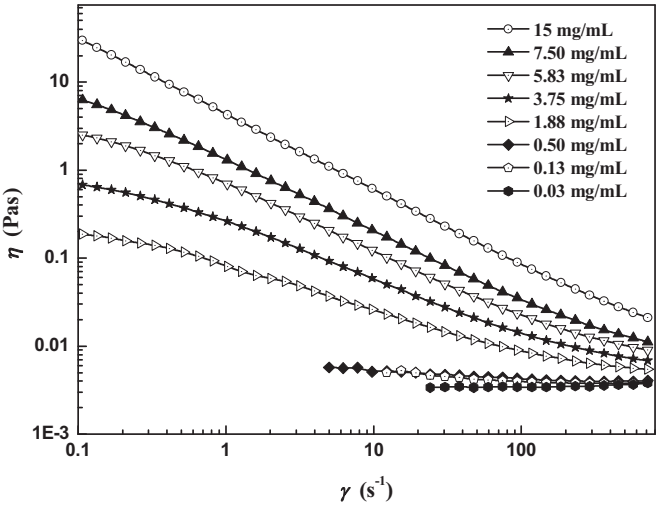

Fig. 1. Dependence of apparent viscosity η on shear rate γ of EPS aqueous solutions at 25 °C. The EPS concentration is 15, 10, 7.50, 5.83, 3.75, 1.88, 0.50, 0.13, 0.03 mg/mL from top to bottom.

decreased with a decrease of c as speculated. At $c \geq 1.88$ mg/mL, Newtonian plateaus of the solutions were not detected even at lower γ, but shear-thinning behavior occurred and became more remarkable at high γ and c. At $c \leq 0.5$ mg/mL, η was almost independent on γ, and the solution was similar to Newtonian fluid.

As described above, Newtonian plateaus of these solutions at $c \geq 1.88$ mg/mL could not be detected even at the lowest γ in the test range. However, it could be expected that Newtonian plateaus should appear when γ was low enough. The γ at which the Newtonian flow changes into shear-thinning behavior is generally defined as critical shear rate (γ_c) (Xu et al., 2008). As indicated by Fig. 1, the γ_c of EPS was lower than 0.1 s^{-1}. At low γ, this shear-thinning behavior was also observed from other polysaccharides, such as xanthan gum, locust bean gum, curdlan, gellan gum, and their values of γ_c were lower than 0.01 s^{-1}, 0.01 s^{-1}, 0.1 s^{-1} and 0.02 s^{-1}, respectively (Mandala, Savvas, & Kostaropoulos, 2004; Silva-Correia et al., 2013; Zhang & Nishinari, 2009). Mandala et al. (2004) also found that xanthan gum had very low γ_c, which was due to its propensity to be orientated under shear because of its extended and semi-rigid conformation. In our case, the extended and rigid chain of EPS in aqueous solution might be oriented easily under shear, leading to the shear-thinning behavior at low γ. Considering the effect of c, each EPS molecule sufficiently extended and randomly separated in dilute solution, so as to the intermolecular interactions could be ignored. The shear-thinning behavior was mainly caused by the orientation of EPS molecules under shear. As for semidilute and concentrated solutions, the low-energy intra- and intermolecular interactions (hydrogen bonds, hydrophobic interactions, van der Waals forces etc.) enhanced and the number of the entanglements among EPS molecular chains increased with increasing c (Xu et al., 2008). The shear-thinning behavior was attributed to the destruction of these intra- and intermolecular interactions as well as orientation of EPS molecules under shear, which led to a more pronounced shear-thinning behavior at high c and γ. The solutions showed typical characteristics of structured fluids or weak gels.

The shear-thinning behavior could be described by cross equation as follows (Zhang et al., 2008):

$$\eta = \eta_\infty + \frac{\eta_0 - \eta_\infty}{1 + K\gamma^n} \quad (3)$$

where η is the apparent viscosity; η_0 is the zero-shear rate viscosity; η_∞ is the infinite shear rate viscosity; γ is the shear rate; K is consistency index and n is the power law index depending on the polymer concentration. Since η_∞ was never approached in this study, Eq. (3) was simplified, assuming $\eta_0 \gg \eta_\infty$.

$$\eta = \frac{\eta_0}{1 + K\gamma^n} \quad (4)$$

Table 1 lists the η_0, K and n of EPS solutions at various c fitted by the simplified cross model (Eq. (4)) together with the magnitudes of relative deviation error (RE). The RE was calculated to be 0–0.3, indicating that the simplified cross equation could describe the shear-thinning behavior well. It can be seen that the η_0, K and n increased with increasing concentration. The η_0 is a macroscopic indicator of the microstructural nature of polymers, and a higher η_0 suggests a greater number of links between the polymer molecules. The parameter K is related to the structural relaxation time, and its increase with c indicates a rising of relaxation time due to an increase in the entanglement density of the polymer chains (Xu et al., 2008). The power law index n reflects the level of shear-thinning behavior. The n values tending to zero represents an increasing Newtonian behavior, while an increasing shear-thinning behavior is indicated by n tending to 1. In this study, the parameter n of EPS solutions increased from 0.008 to 0.84 with c increased from 0.03 to 15 mg/mL, indicating an increasing shear-thinning behavior for EPS solutions. It has been reported that the value of n will be ca. 0.72 for the entanglement network, but ca. 0.9 for the "weak gel" (Xu et al., 2007). Moreover, a higher n value demonstrates the presence of interchain interaction in the semi- and concentrated solution regions. Therefore, it can be speculated that the EPS solutions might form an entanglement network or even gelate at high concentration through inter-chain interaction.

3.3. Concentration dependence of the zero-shear viscosity in steady shear

Fig. 2 shows the concentration dependence of η_0 for EPS aqueous solutions at 25 °C. Obviously, the η_0 deviated from the linear dependence of viscosity on c. By fitting the experimental data using power law equations, three concentration regions (dilute, semidilute and concentrated region) were determined. In the dilute region, a slope of ca. 1.00 was obtained from a logarithmic plot of η_0 vs c. In this region, individual polymeric coils are randomly separated, and only intramolecular hydrodynamic interactions within individual macromolecules may occur. The linear increase in viscosity with increasing c results from the Brownian motion of the chains and perturbation of solvent flow caused by individual coils (Goh, Hemar, & Singh, 2005). As c increased, a higher slope of 2.60 was obtained in the semidilute region. Random polymer molecules started to overlap and interpenetrate each other to form

Table 1
Magnitudes of the cross model parameters for steady simple shearing, obtained for exopolysaccharide (EPS) at various concentration.

Concentration (mg/mL)	η_0 (Pa s)	K (s^n)	n	RE
15	310.3	62.02	0.84	0.14
10	126.5	23.20	0.83	0.23
7.50	17.80	10.42	0.74	0.34
5.83	6.11	6.93	0.68	0.33
3.75	1.75	5.61	0.57	0.26
1.88	0.68	7.08	0.43	0.21
0.50	0.0092	0.83	0.07	0.05
0.13	0.0055	0.28	0.08	0.06
0.03	0.0023	0.33	0.008	0.04

RE, relative deviation error $= \sum_{i=1}^{n} \frac{\left(\left|(x_{\exp,i} - x_{\mathrm{cal},i})/x_{\exp,i}\right|\right)}{n}$

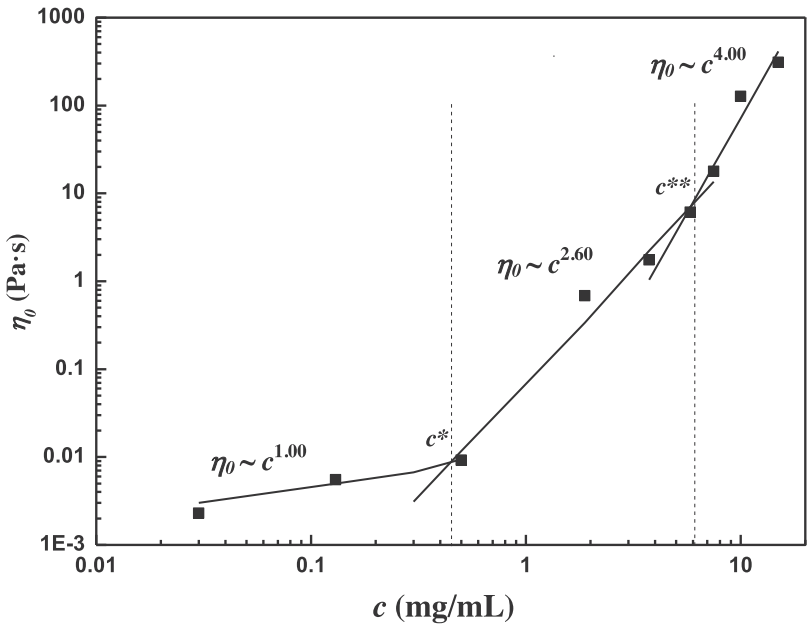

Fig. 2. Dependence of zero-shear viscosity η_0 on concentration c for EPS aqueous solutions at 25 °C.

more physical entanglements, as a result of a significant increase in viscosity. With a further increase of c, the slope increased to 4.00 in the concentrated region. The number of the junctions between EPS molecules increased further, and a relatively stable gel network might be generated, leading to a dramatic increase in viscosity. When the slope increased from 1.00 to 2.60 and even to 4.00, the two critical concentrations (c^* and c^{**}) for the transition from dilute to semidilute and to concentrated solution were 0.45 mg/mL and 6.14 mg/mL, respectively.

3.4. Temperature dependence of apparent viscosity in steady shear

To investigate the effect of temperature on viscosity of EPS solutions, steady shear measurements for the EPS solutions at 3.75 and 7.50 mg/mL were performed at 4, 10, 15, 20, 25 and 35 °C, respectively. The temperature dependence of η at each EPS concentration was evaluated by Arrhenius equation:

$$\eta = A\exp^{(Ea/RT)} \quad (5)$$

where Ea is the flow activation energy; A is the frequency factor and R is the gas constant, 8.314 J/mol K. Fig. 3 illustrates that the relationship between the η of EPS solutions and T at the two concentrations generally obeys the Arrhenius equation. Based on the slope of the plots of lnη vs 1000/T, Ea was calculated to be 8.67, 7.23 and 5.92 kJ/mol for 3.75 mg/mL EPS solution, and 3.35, 2.48 and 1.83 kJ/mol for 7.50 mg/mL EPS solution at 0.5, 1 and 2 s^{-1}, respectively. Obviously, Ea decreased with the increase of c and γ in the test range. It was reported that the Ea of xanthan and gelatin decreased with increasing c in line with our results, while the Ea of carrageenan, starch and chitosan increased with increasing c, and the Ea of pectin increased with c up to the maximum at 3 wt%, followed by a decrease (Desbrieres, 2002; Marcotte, Taherian Hoshahili, & Ramaswamy, 2001). Interestingly, Xu et al. (2007) found that the Ea of *Aeromonas* gum aqueous solution was independent on c from 4.88 wt% to 6.05 wt%. Therefore, it can be concluded that the effects of temperature on viscosity are various for different polymers, which is closely related to their inherent characteristics of structure. As for EPS solutions, the number of the junctions between EPS molecules increased with increasing c, and EPS solutions tended to form a stable gel network. Consequently, the EPS became less sensitive to temperature, as indicated by a smaller Ea. In addition, under slightly higher shear it was easier for EPS molecules to orientate and form an order structure, which could also lead to a decrease in Ea.

3.5. Angular frequency and concentration dependence of G', G'' and η^* in dynamic frequency sweep

In dynamic oscillatory tests, the G' and G'' represent the elasticity and viscosity of samples, respectively. The dependence of G' and G'' on ω can be used to characterize a dispersion system by four most common classifications, which are a dilute solution, an entanglement network, a weak gel and a strong gel. A dilute solution shows G'' higher than G' over the entire frequency range (Nishinari, 1997). A entanglement network shows G' and G'' curves intersecting in the test frequency range, suggesting a clear tendency of more solid-like behavior at higher frequencies (Xu et al., 2008). A weak gel shows G' larger than G'', and both of them almost parallel to each other. A strong gel also shows G' larger than G'', but the slope of G' curve approaches to 0 and G'' has a minimum at intermediate frequencies (Chenite, Buschmann, Wang, Chaput, & Kandani, 2001; Moreira et al., 2014). Fig. 4 shows the G' and G'' as a function of ω for EPS at various c and 25 °C. Both G' and G'' were strongly frequency-dependent. In the low and intermediate frequency range, the G' and G'' for all EPS solutions increased with increasing ω. Moreover, the effect of c on the two moduli was significant. When c = 1.25 mg/mL, the G'' was throughout higher than G', and the solution was predominately liquid-like over the entire frequency range studied. As c increased to 3.75 and 5.00 mg/mL, there was a crossover between G' and G'' in the low frequency range, and the cross point shifted to low ω with increasing c, as labeled with arrows in Fig. 4. When $c \geq$ 7.50 mg/mL, G' was always greater than G'' in the low and intermediate frequency range, and the two moduli nearly parallelled to each other. Based on the classifications mentioned above, the EPS solution of 1.25 mg/mL should be classified as a dilute solution, while the EPS solutions of 3.75 and 5.00 mg/mL formed entanglement network, and other EPS solutions at higher c ($\geq$7.50 mg/mL) established weak gel structures.

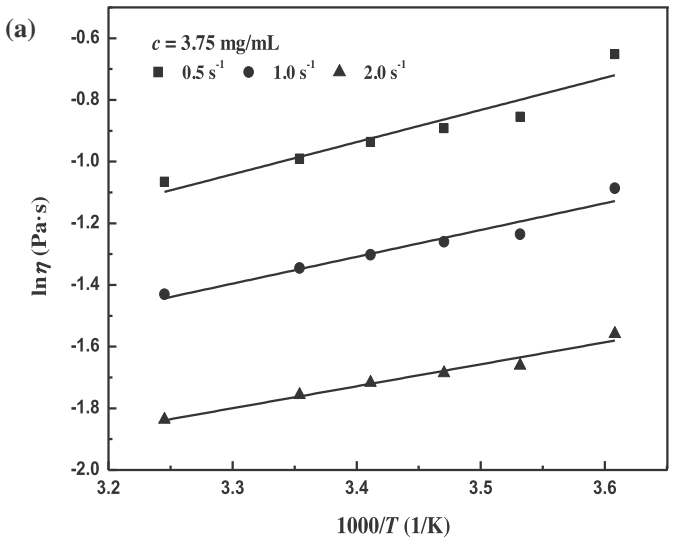

Fig. 3. Arrhenius plots for apparent viscosity η of EPS aqueous solutions at two concentrations of 3.75 mg/mL (a) and 7.50 mg/mL (b) with three shear rates of 0.5, 1.0 and 2.0 s^{-1}.

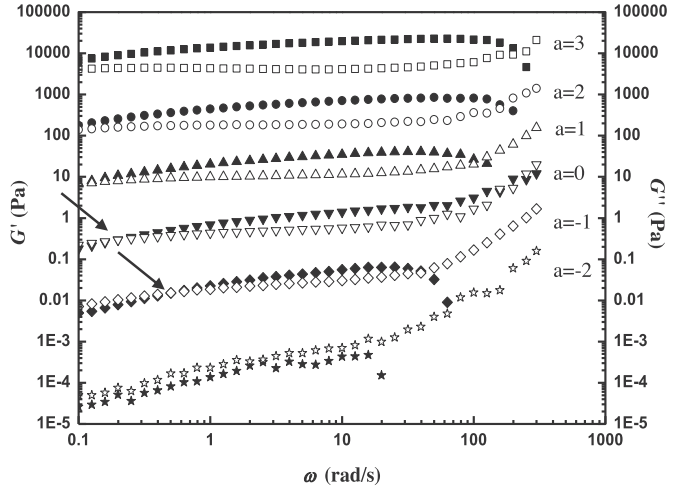

Fig. 4. Plots of storage modulus G' (solid symbols) and loss modulus G'' (open symbols) vs angular frequency ω for EPS at different concentrations and 25 °C. The EPS concentration is 1.25, 3.75, 5.00, 7.50, 10 and 15 mg/mL from bottom to top. The data were shifted along vertical axes by 10^a to avoid overlapping.

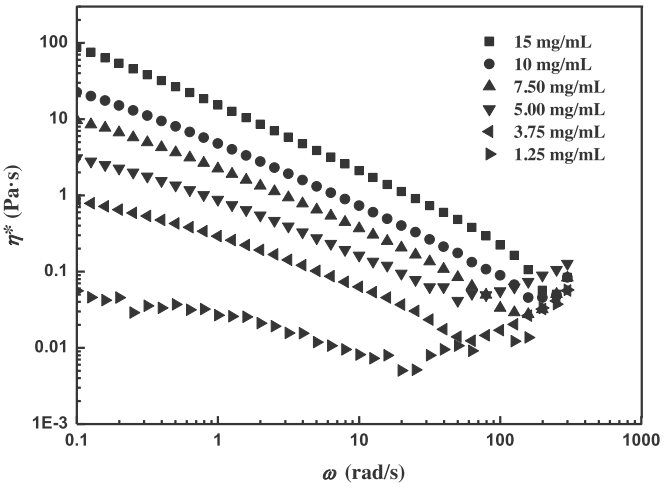

Fig. 5. Plots of complex viscosity η^* vs angular frequency ω for EPS aqueous solutions at different concentrations and 25 °C.

It is interesting that, in the high frequency range ($\omega > 50$ rad/s), G' dropped while G'' increased dramatically except for that of 1.25 mg/mL EPS solution. Consequently, the two moduli crossed at a certain ω. Moreover, the crossover of G' and G'' exhibited a shift to high ω with increasing c. It was reported that the G' of ice cream mix (ICM) increased initially with increasing oscillation frequency, followed by a decrease, and the ω at which G' began to decrease became lower with increasing temperature (Dogan, Kayacier, Toker, Yilmaz, & Karaman, 2013; Toker et al., 2013). Similar phenomenon was also found on gellan gum and guar/xanthan mixed gum (Pal, 1996; Silva-Correia et al., 2013). However, why G' decreased dramatically and intersected with G'' at high ω still needs a further research. In this study, it can be speculated that the junctions formed by weak interaction between molecules were broken under high frequency oscillating stress, leading to the decrease in elastic response G' and increase in viscous response G''. Moreover, with increasing c, the number and strength of the junctions between molecules increased, so that the frequency oscillating stress was high enough to break these junctions, which led to an increase of the ω at which G' and G'' intersected.

Fig. 5 shows the η^* as a function of ω for EPS at various c and 25 °C. The η^* values of these solutions decreased with increasing ω in low and intermediate frequency range, and the decrease in η^* became

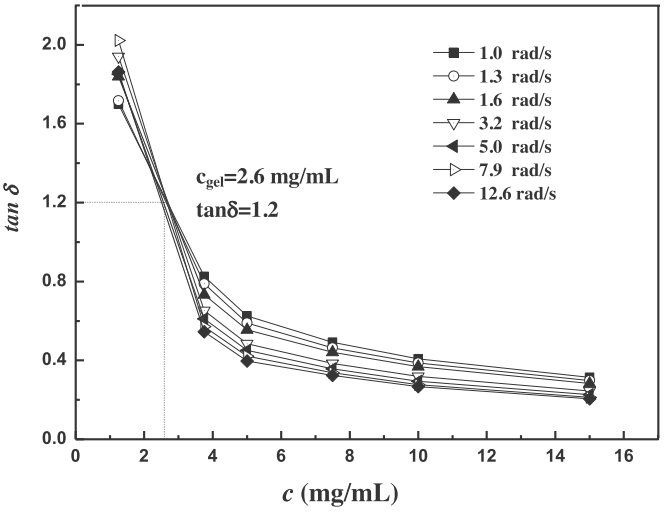

Fig. 6. Loss tangent tanδ as a function of concentration c for EPS aqueous solutions at different frequencies and 25 °C.

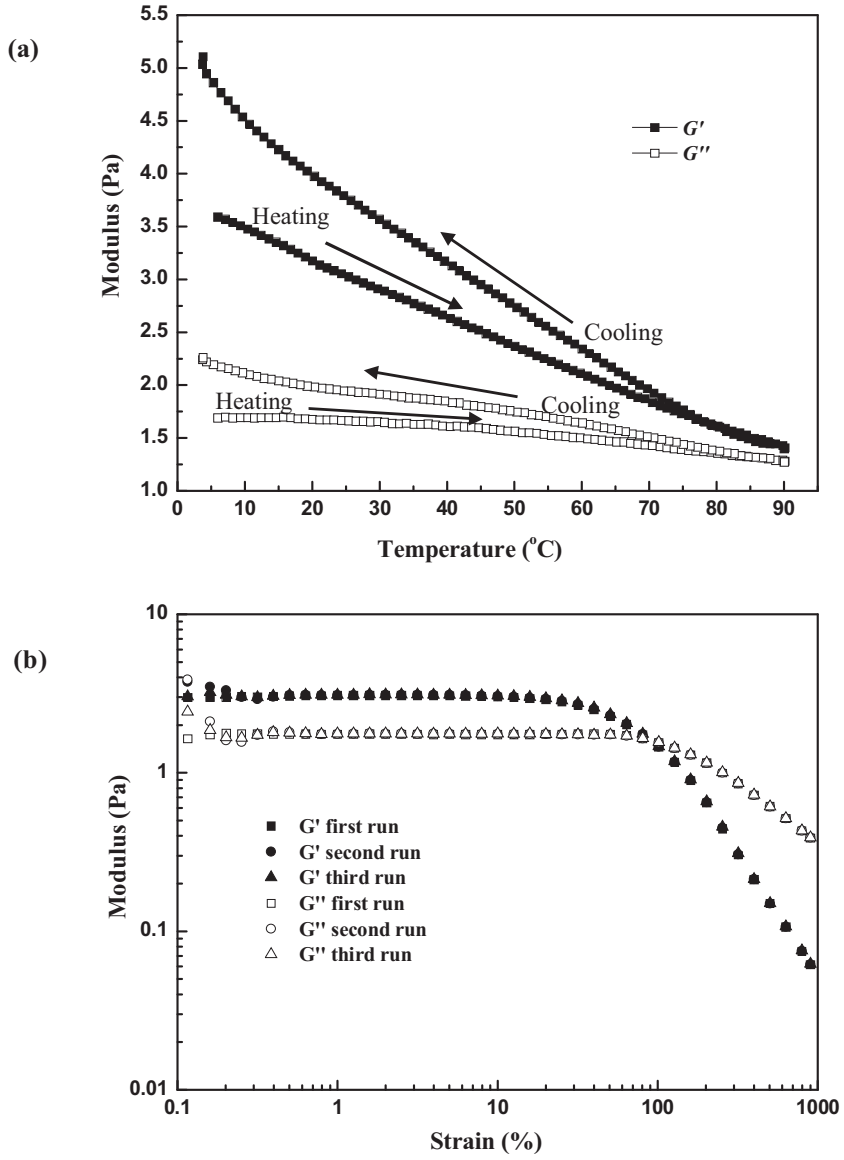

Fig. 7. Plots of storage modulus G' (solid symbols) and loss modulus G'' (open symbols) for 10 mg/mL EPS aqueous solutions in temperature ramp (a) and strain sweep measurements (b).

more obvious at higher c. However, the η^* rose up with increasing ω in high frequency range, and the rising of η^* was more apparent at lower c. Furthermore, the ω at which η^* began to rise showed a shift to high ω with increasing c. Zhang and Nishinari (2009) reported that the extensional viscosity (η_E) of curdlan in DMSO decreased initially with increasing strain rate, followed by an increase. The first drop in η_E, namely strain-thinning, was due to the mechanical destruction of intermolecular entanglement. Moreover, the disentanglement had more contribution to the decrease of viscosity in concentrated solutions compared with in dilute solutions, which caused the strain-thinning behavior more apparent in concentrated solutions. The increase in η_E, namely strain-thickening, might be attributed to a large drag generated by the stretching and orientation of the chains under high strain rate. In this study on EPS, the decrease in η^* (shear-thinning) in low and intermediate frequencies was attributed to the intermolecular entanglement disruption caused by oscillating shear stress. The disentanglement of EPS molecule chains had more contribution to the decrease of viscosity in concentrated solutions, so more obvious decrease in η^* was observed at higher c. The increase in η^* (shear-thickening) in high frequency range was due to the stretching and orientation of EPS molecules as well as a large flow resistance resulted from the rigid chains. The shear-thickening behavior mainly reflects the inherent structure characteristics of EPS as an extended and rigid chain other than the fluid mechanic effects. In addition, since intermolecular entanglement was more serious in concentrated solutions than in dilute ones, a higher frequency shear stress was necessary for entire disentanglement in concentrated solutions, indicating that the critical frequency, at which shear-thickening behavior was started, tended to high ω with increasing c.

3.6. Determination of critical gelation concentration

To determine the gel point is important for studying a gel system. At present, Winter–Chambon criterion has been proved to be a valid and reliable approach to determine the gel point of polymers (Pogodina & Winter, 1998). According to the criterion, the gel point is identified as the critical point at which the modulus G' and G'' scale in an identical fashion with frequency. Namely, the G' and

G'' of a critical gel obey a power law with the same exponent n as follows:

$$G'(\omega) \sim G''(\omega) \propto \omega^n \quad 0 < n < 1 \tag{6}$$

or

$$\frac{G''(\omega)}{G'(\omega)} = \tan\delta = \tan\left(\frac{n\pi}{2}\right) \tag{7}$$

where tanδ is loss tangent. The frequency-independence of tanδ in the vicinity of gel point has been widely employed to determine the gel point such as the critical gelation time, temperature and concentration (Liu, Zhang, He, & Hu, 2003).

Fig. 6 shows a multifrequency plot of tanδ vs c for EPS aqueous solutions at 25 °C. All curves at different frequencies exhibited a similar trend of decrease in tanδ with increasing c, indicating that gel structure was formed and enhanced. Furthermore, each curve passed through the common point at a certain c; the cross point was known as gel point, at which tanδ showed frequency-independence, and the corresponding concentration was defined as the critical gelation concentration (c_{gel}) (Liu et al., 2003). With respect to EPS, c_{gel} was estimated to be 2.6 mg/mL and the corresponding tanδ was 1.2 at 25 °C. The critical exponent n was calculated as 0.56 by Eq. (7). The c_{gel} for EPS was lower than that of other polymers at 25 °C, such as alginate (20 mg/mL), polyvinyl chloride (12.5 mg/mL) and lentinan (4 mg/mL) (Li & Aoki, 1997; Lu, Liu, Dai, & Tong, 2005; Zhang et al., 2008). The relatively low c_{gel} indicates a strong gel forming ability for EPS at room temperature. Moreover, c_{gel} was higher than c^*, but lower than c^{**}, suggesting that the EPS solution at gel point was located in semidilute region, which further confirms that the gelation resulted from the overlapping and interpenetrating of polymer molecules to form entanglement network.

3.7. Evaluation of gel properties by temperature ramp and strain sweep tests

To evaluate the gel properties formed by EPS solutions, the EPS solution at the concentration of 10 mg/mL was examined through temperature ramp test and strain sweep test. Fig. 7(a) shows the dependence of G' and G'' on temperature during heating and cooling. In spite of heating and cooling, the G' higher than G'' throughout test temperature range indicated that gel had formed in 10 mg/mL EPS solutions, which can be confirmed by c_{gel} 2.6 mg/mL. Obviously, G' and G'' decreased during heating, while increased during subsequent cooling. The curves of G' and G'' during heating did not overlap with those during cooling, but were lower than those during cooling, indicating that the impact of temperature on EPS gel structure is irreversible and cooling was favorable for the enhancement of gel network due to the aggregation of the rigid chains of EPS (Nishinari & Takahashi, 2003).

Fig. 7(b) shows the dependence of G' and G'' on strain at 25 °C. The strain sweep was replicated 3 times, and the next sweep was started immediately after the previous one was finished. The G' and G'' kept constant until the strain surpassed 10%. Once the strain was larger than 10%, G' and G'' showed a sharp drop, which could be attributed to the disruption of gel network structure caused by a large strain. Thereby, the upper limit of the linear viscoelastic range for EPS solutions was 10% of strain. Moreover, the G' and G'' curves of the second and third run overlapped with those of the first run, indicating that the EPS gel was strain-reversible. The network structure in EPS gels should not be permanent, which could recover soon even though it had been destroyed during the previous strain sweep (Guo, Cui, Wang, Goff, & Smith, 2009). Hence, it could be concluded that the formation of the network structure of EPS gels was due to the loose junctions formed by intermolecular entanglement and that the loose junctions were strain-reversible, indicating that EPS gels had typical characteristics of weak gel.

4. Conclusions

The rheological behaviors of EPS were studied in this study. The [η] of EPS was 1986 ± 55 mL/g in pure water similar to that in 0.2 M NaCl (1990 ± 175 mL/g), indicating that EPS is a neutral polysaccharide and existed as an extended and rigid chain in aqueous solution. The steady shear indicated that EPS solutions showed shear-thinning behavior even at low γ of 0.1 s^{-1} and became apparent with increasing c. From the c dependence of η_0 calculated by cross model, two critical transition concentrations (c^* and c^{**}) from a dilute solution to semidilute and then to concentrated domain were 0.45 mg/mL and 6.14 mg/mL. The Ea calculated by Arrhenius equation decreased with increasing c and γ, indicating a lower sensitivity to temperature resulted from gelation. From dynamic frequency sweep, the EPS system was classified to three regions, i.e., dilution solution (1.25 mg/mL), entanglement network (3.75 and 5.00 mg/mL) and weak gel (7.50, 10 and 15 mg/mL). In the later two regions, G' increased with increasing ω in low and intermediate frequency range, whereas it dropped and intersected with G'' in high frequency range, suggesting that the junctions formed by weak interaction between EPS molecules were broken under high-frequency oscillating stress. Interestingly, the increase of η^* occurred in high frequency range due to the stretching and orientation of EPS molecules as well as a large flow resistance resulted from the extended and rigid chain. This shear-thickening behavior reflects the inherent structure characteristics of EPS with an extended and rigid chain rather than the fluid mechanic effects. According to Winter–Chambon criterion, c_{gel} was calculated to be 2.6 mg/mL lower than that of general polymers, suggesting a strong gelation ability of EPS at room temperature. Temperature ramp measurements showed that the gel formed by 10 mg/mL EPS solution was temperature-irreversible and enhanced by cooling due to the aggregation of rigid chains at low temperature. Repetitive strain sweeps showed that the G' and G'' curves for three runs overlapped with each other, indicating that the EPS gel was strain-reversible. The EPS gel network was not permanent and had typical characteristics of weak gel.

Acknowledgements

This work was supported by National Natural Science Foundation of China (31401652), and Application and Foundation Research Project of Wuhan Science and Technology Bureau of China (2014020101010068).

Appendix A. Supplementary data

Supplementary data associated with this article can be found, in the online version, at http://dx.doi.org/10.1016/j.carbpol.2014.08.055.

References

Chenite, A., Buschmann, M., Wang, D., Chaput, C., & Kandani, N. (2001). Rheological characterisation of thermogelling chitosan/glycerol-phosphate solutions. *Carbohydrate Polymers*, *46*(1), 39–47.

Desbrieres, J. (2002). Viscosity of semiflexible chitosan solutions: Influence of concentration, temperature, and role of intermolecular interactions. *Biomacromolecules*, *3*(2), 342–349.

Dogan, M., Kayacier, A., Toker, O. S., Yilmaz, M. T., & Karaman, S. (2013). Steady, dynamic, creep, and recovery analysis of ice cream mixes added with different concentrations of xanthan gum. *Food and Bioprocess Technology*, *6*, 1420–1433.

Funami, T., Funami, M., Yada, H., & Nakao, Y. (2000). A rheological study on the effects of heating rate and dispersing method on the gelling characteristics of curdlan aqueous dispersions. *Food Hydrocolloids*, *14*, 509–518.

Goh, K. K. T., Hemar, Y., & Singh, H. (2005). Viscometric and static light scattering studies on an exopolysaccharide produced by *Lactobacillus delbrueckii subspecies bulgaricus* NCFB 2483. *Biopolymers*, *77*(2), 98–106.

Guo, Q., Cui, S. W., Wang, Q., Goff, H. D., & Smith, A. (2009). Microstructure and rheological properties of psyllium polysaccharide gel. *Food Hydrocolloids*, *23*(6), 1542–1547.

Higiro, J., Herald, T. J., & Alavi, S. (2006). Rheological study of xanthan and locust bean gum interaction in dilute solution. *Food Research International*, *39*(2), 165–175.

Huang, Q. L., Siu, K. C., Wang, W. Q., Cheung, Y. C., & Wu, J. Y. (2013). Fractionation, characterization and antioxidant activity of exopolysaccharides from fermentation broth of a *Cordyceps sinensis* fungus. *Process Biochemistry*, *48*(2), 380–386.

Huang, Z. P., Huang, Y. N., Li, X. B., & Zhang, L. N. (2009). Molecular mass and chain conformations of *Rhizoma Panacis Japonici* polysaccharides. *Carbohydrate Polymers*, *78*(3), 596–601.

Li, L., & Aoki, Y. J. (1997). Rheological images of poly(vinyl chloride) gels. 1. The dependence of sol–gel transition on concentration. *Macromolecules*, *30*(25), 7835–7841.

Liu, C. Y., Zhang, J., He, J. S., & Hu, G. H. (2003). Gelation in carbon nanotube/polymer composites. *Polymer*, *44*(24), 7529–7532.

Lu, L., Liu, X. X., Dai, L., & Tong, Z. (2005). Difference in concentration dependence of relaxation critical exponent n for alginate solutions at sol–gel transition induced by calcium cations. *Biomacromolecules*, *6*(4), 2150–2156.

Mandala, I. G., Savvas, T. P., & Kostaropoulos, A. E. (2004). Xanthan and locust bean gum influence on the rheology and structure of a white model-sauce. *Journal of Food Engineering*, *64*(3), 335–342.

Marcotte, M., Taherian Hoshahili, A. R., & Ramaswamy, H. S. (2001). Rheological properties of selected hydrocolloids as a function of concentration and temperature. *Food Research International*, *34*(8), 695–703.

Moreira, H. R., Munarin, F., Gentilini, R., Visai, L., Granja, P. L., Tanzi, M. C., et al. (2014). Injectable pectin hydrogels produced by internal gelation: pH dependence of gelling and rheological properties. *Carbohydrate Polymers*, *103*, 339–347.

Nishinari, K. (1997). Rheological and DSC study of sol–gel transition in aqueous dispersions of industrially important polymers and colloids. *Colloid and Polymer Science*, *275*(12), 1093–1107.

Nishinari, K., & Takahashi, R. (2003). Interaction in polysaccharide solutions and gels. *Current Opinion in Colloid & Interface science*, *8*(4), 396–400.

Pal, R. (1996). Rheological properties of mixed polysaccharides and polysaccharide-thickened emulsions. *AIChE Journal*, *42*(7), 1824–1832.

Pogodina, N. V., & Winter, H. H. (1998). Polypropylene crystallization as a physical gelation process. *Macromolecules*, *31*(23), 8164–8172.

Silva-Correia, J., Gloria, A., Oliveira, M. B., Mano, J. F., Oliveira, J. M., Ambrosio, L., et al. (2013). Rheological and mechanical properties of acellular and cell-laden methacrylated gellan gum hydrogels. *Journal of Biomedical Materials Research A: Applied Biomaterials*, *101*(12), 3438–3446.

Toker, O. S., Karaman, S., Yuksel, F., Dogan, M., Kayacier, A., & Yilmaz, M. T. (2013). Temperature dependency of steady, dynamic, and creep-recovery rheological properties of ice cream mix. *Food and Bioprocess Technology*, *6*(11), 2974–2985.

Wang, L., Wang, G. Y., Zhang, J. J., Zhang, G. Q., Jia, L., Liu, X. N., et al. (2011). Extraction optimization and antioxidant activity of intracellular selenium polysaccharide by *Cordyceps sinensis* SU-02. *Carbohydrate Polymers*, *86*(4), 1745–1750.

Wang, Z. M., Peng, X. A., Lee, K. L. D., Tang, J. C. O., Cheung, P. C. K., & Wu, J. Y. (2011). Structural characterisation and immunomodulatory property of an acidic polysaccharide from mycelial culture of *Cordyceps sinensis* fungus Cs-HK1. *Food Chemistry*, *125*(2), 637–643.

Wu, D. T., Meng, L. Z., Wang, L. Y., Lv, G. P., Cheong, K. L., Hu, D. J., et al. (2014). Chain conformation and immunomodulatory activity of a hyperbranched polysaccharide from *Cordyceps sinensis*. *Carbohydrate Polymers*, *110*, 405–414.

Xu, S. Q., Xu, X. J., & Zhang, L. N. (2012). Branching structure and chain conformation of water-soluble glucan extracted from *Auricularia auricula-judae*. *Journal of Agricultural and Food Chemistry*, *60*(13), 3498–3506.

Xu, X. J., Chen, P., & Zhang, L. N. (2007). Viscoelastic properties of an exopolysaccharide: Aeromonas gum, produced by *Aeromonas nichidenii* 5797. *Biorheology*, *44*(5), 387–401.

Xu, X. J., Xu, J., Zhang, Y. Y., & Zhang, L. N. (2008). Rheology of triple helical Lentinan in solution: Steady shear viscosity and dynamic oscillatory behavior. *Food Hydrocolloids*, *22*(5), 735–741.

Yan, J. K., Wang, W. Q., & Wu, J. Y. (2014). Recent advances in *Cordyceps sinensis* polysaccharides: Mycelial fermentation, isolation, structure, and bioactivities: A review. *Journal of Functional Foods*, *6*, 33–47.

Yoshimura, M., & Nishinari, K. (1999). Dynamic viscoelastic study on the gelation of konjac glucomannan with different molecular weight. *Food Hydrocolloids*, *13*, 227–233.

Zhang, H. B., & Nishinari, K. (2009). Characterization of the conformation and comparison of shear and extensional properties of curdlan in DMSO. *Food Hydrocolloids*, *23*(6), 1570–1578.

Zhang, Y. Y., Li, S., Wang, X. H., Zhang, L. N., & Cheung, P. C. K. (2011). Advances in lentinan: Isolation, structure, chain conformation and bioactivities. *Food Hydrocolloids*, *25*(2), 196–206.

Zhang, Y. Y., Xu, X. J., & Zhang, L. N. (2008). Gel formation and low-temperature intramolecular conformation transition of a triple-helical polysaccharide lentinan in water. *Biopolymers*, *89*(10), 852–861.

Zhao, J., Xie, J., Wang, L. Y., & Li, S. P. (2014). Advanced development in chemical analysis of *Cordyceps*. *Journal of Pharmaceutical and Biomedical Analysis*, *87*, 271–289.